

Deep Structure of Arc Volcanoes as Inferred from Seismic Observations

A. Hasegawa, A. Yamamoto, D. Zhao, S. Hori and S. Horiuchi

Phil. Trans. R. Soc. Lond. A 1993 **342**, 167-178

doi: 10.1098/rsta.1993.0012

Email alerting service

Receive free email alerts when new articles cite this article - sign up in the box at the top right-hand corner of the article or click [here](#)

To subscribe to *Phil. Trans. R. Soc. Lond. A* go to:
<http://rsta.royalsocietypublishing.org/subscriptions>

Deep structure of arc volcanoes as inferred from seismic observations

BY A. HASEGAWA¹, A. YAMAMOTO¹, D. ZHAO², S. HORI¹ AND S. HORIUCHI¹

¹ *Observation Center for Prediction of Earthquakes and Volcanic Eruptions, Faculty of Science, Tohoku University, Sendai 980, Japan*

² *Geophysical Institute, University of Alaska Fairbanks, Fairbanks, Alaska 99775, U.S.A.*

Possible evidence for deep-seated magmatic activity beneath the northeastern Japan arc has been obtained from micro-earthquake observations. Tomographic inversions for *P*-wave velocity clearly delineate low-velocity zones, which are inclined to the west and continuously distributed from the uppermost mantle to the upper crust beneath active volcanoes. Exceptionally deep (22–40 km) micro-earthquakes are found at 10 locations around the low-velocity zones beneath active volcanoes. All these events have extremely low predominant frequencies, suggesting a close relation to the magmatic activity in this depth range. At shallower depths (8–15 km) distinct reflectors of *S*-waves from shallow events are found at five locations in or around the low-velocity zones. Their locations and reflection coefficients suggest that the reflectors are very thin magma bodies existing in the mid-crust. These observations shed some light on the state of magma at depths beneath volcanic arcs.

1. Introduction

Northeastern Japan is located at a typical subduction zone, where the oceanic Pacific plate subducts under the continental plate at an angle of about 30°. Many shallow earthquakes occur beneath the Pacific Ocean between the Japan trench and the Pacific coast, most of them originating at the boundary of the two converging plates. The shallow seismicity along the plate boundary is continuous with the deep seismic zone, which is within the subducted Pacific plate and attains a depth of about 650 km. The deep seismic zone, down to a depth of about 150 km, is composed of two thin planes which are parallel to each other and are 30–40 km apart. Very shallow earthquakes, confined to the upper crust, occur beneath the land area, although their activity is not very high. Active volcanoes are distributed in the land area, mainly along the volcanic front which runs through the middle of the land area almost parallel to the trench axis.

The seismic network of Tohoku University covers this tectonically active area. Seismic signals from high-gain short-period three-component seismic stations are centrally recorded on digital magnetic tape at the observation centre in Sendai by using telephone telemetry, which facilitates accurate hypocentre location of micro-earthquakes occurring in this area and enables us to accurately estimate the seismic velocity structure of the crust and upper mantle beneath this area. Detailed studies on seismic activity and on the crust and upper mantle structure, recently made by using data obtained from this network, show some evidence for magmatic activity in the crust and upper mantle. In the present paper we describe briefly the results of

Phil. Trans. R. Soc. Lond. A (1993) **342**, 167–178

© 1993 The Royal Society

Printed in Great Britain

167

these studies on deep structure of active volcanoes beneath this area, the northeastern Japan arc, based on the seismic observations.

2. Low-velocity zones beneath active volcanoes

Many tomographic studies on local or regional scale have been carried out in various areas of the world since the pioneering works of seismic tomography by Aki & Lee (1976) and Aki *et al.* (1977). In subduction zones, the most extensive studies have been made in the Japan Islands. Hirahara *et al.* (1989) investigated the *P*-wave velocity structure beneath central Japan, and found low-velocity zones in the wedge mantle above the high-velocity Pacific plate subducted beneath this region. One of these low-velocity bodies coincides with an S-wave anisotropic body detected by Ando *et al.* (1983). Tomographic studies by Hasemi *et al.* (1984) and Obara *et al.* (1986) in northeastern Japan reveal *P*-wave low-velocity zones existing in the crust and in the wedge mantle just beneath active volcanoes.

The results of these studies show that tomographic studies play an important part for a deeper understanding of arc volcanism. In these studies, however, there still remain the following problems as in most of the conventional tomographic studies. It is known that there exist seismic velocity discontinuities, such as the Moho and Conrad discontinuities and the upper boundary of the subducted slab, in the crust and upper mantle beneath the northeastern Japan arc. However they do not take into consideration the effect of the complicated-shaped discontinuities or even their existence, which distorts the estimated tomographic images especially in the vicinity of the discontinuities. Another problem is that three-dimensional (3D) ray tracing is not used to calculate seismic ray paths and travel times. In very heterogeneous regions, such as subduction zones, calculated ray paths based on a simple 1D velocity model deviate considerably from the real paths in large hypocentral distances; this again seriously distorts the final tomographic images.

We developed a new tomographic method to solve the above-mentioned problems (Zhao *et al.* 1992). This method copes with a general velocity structure with complicated-shaped velocity discontinuities in the modelling space and with 3D variations in the seismic velocity in each layer bounded by the velocity discontinuities. An efficient 3D ray tracing algorithm is developed, which calculates ray paths and travel times very rapidly and accurately for *P* and *S* waves in a complicated velocity structure as described above. The present method can include in the inversion not only arrival time data of first *P* and *S* waves but also those of later phases such as reflected or converted waves at the velocity discontinuities. Details of the method are described in Zhao *et al.* (1992).

P-wave tomographic images of the crust and upper mantle beneath the northeastern Japan arc are obtained by applying the method to arrival time data of first *P* and *S* waves and *PS* and *SP* waves converted at the velocity discontinuities (Hasegawa *et al.* 1991; Zhao *et al.* 1992). The data used are those observed by the seismic networks of Tohoku University and several other national universities in Japan. This study has updated the tomographic images of the northeastern Japan arc by Hasemi *et al.* (1984) and Obara *et al.* (1986) by covering a wider area and by improving the resolution. The estimated 3D *P*-wave velocity structure is drawn with light and shade on vertical cross sections (figure 1), and on a horizontal plane (figure 2). Figure 1 shows three vertical cross sections of fractional *P*-wave velocity perturbations (in percent) along the lines AA', BB' and CC' in the inset map, which

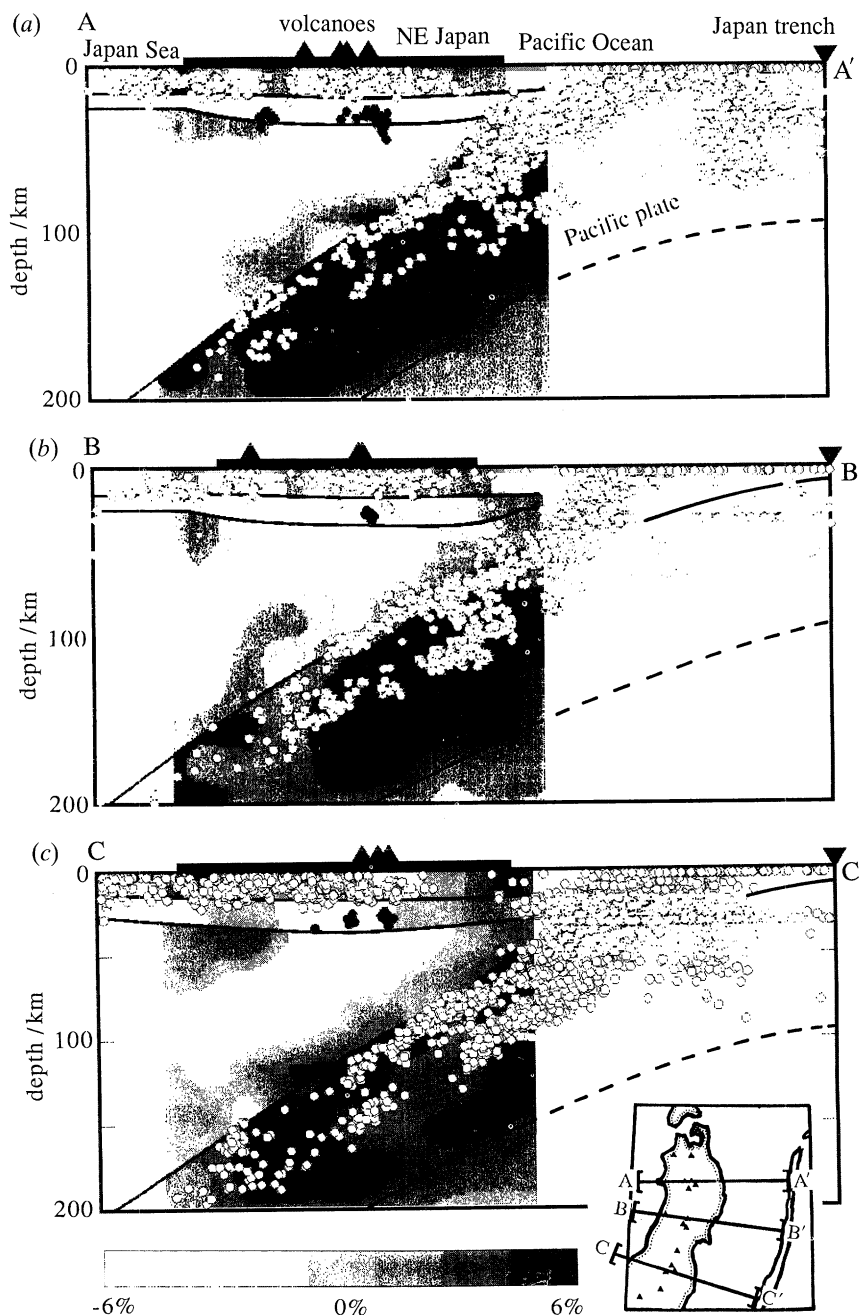


Figure 1. Vertical cross sections of fractional P -wave velocity perturbation (as %) along the lines (a) AA', (b) BB' and (c) CC' in the insert map. Velocity perturbation is shown by the light and shade scale at the bottom. Open circles are micro-earthquakes within a 60 km width along each line located in 1987–90, and solid circles denote low-frequency micro-earthquakes located in 1975–90. The locations of the land area, trench axis and active volcanoes are shown on the top by a thick horizontal line, inverted solid triangles and solid triangles, respectively. The Conrad and Moho discontinuities and the top of the subducted slab, which are fixed in the inversion, are shown by thick lines. The estimated location of the bottom of the slab is also shown by a thick line.

are nearly perpendicular to the trench axis. Figure 2 shows the fractional P -wave velocity perturbations at a depth of 40 km. The velocity perturbation is from the mean value of estimated velocities at each depth, and the perturbation scale is from -6% to 6% . Light and shaded areas correspond to low and high velocities, respectively. In figure 1*a–c*, shown by circles are micro-earthquakes within a 60 km width along each line located by the seismic network of Tohoku University. Also shown by thick curves are the locations of the Conrad and Moho discontinuities and the upper boundary of the subducted Pacific plate, which are fixed in the inversion.

As seen from figure 1, a high-velocity zone corresponding to the subducted Pacific plate is clearly delineated in all the three vertical sections. The lower boundary of this high-velocity zone can be recognized. The location of the lower boundary presently estimated is shown by a solid (and broken) curve in the figure. The thickness of the high-velocity Pacific plate is estimated as 80–90 km. This is in close agreement with an estimation by Umino *et al.* (1991), who detected a reflected and S to P converted phase at the bottom of the subducted Pacific plate in seismograms of intermediate-depth events occurring within the plate. They estimated the thickness of the plate to be *ca.* 85 km based on arrival time analyses of this phase. Figure 1 also shows that the double-planed deep seismic zone (Hasegawa *et al.* 1978) is located within the upper half of the high-velocity Pacific plate.

It is obvious from figure 2 that most of the active volcanoes (solid triangles) are located just above the low-velocity zones in the uppermost mantle. The low-velocity zones are also distributed in the crust just beneath active volcanoes; this is partly seen in figure 1. The low-velocity zones just beneath active volcanoes (solid triangles in figure 1) in the crust and in the uppermost mantle dip to the west in the mantle wedge and extend to a depth of about 150 km. They are approximately parallel to the dip of the subducted Pacific plate. This feature is common to all the low-velocity zones in the crust and in the mantle wedge shown in figure 1*a–c*.

3. Cut-off depth for shallow inland seismicity

In the northeastern Japan arc very shallow earthquakes occur beneath the land area, although the activity of these crustal events is secondary to the major activity along the plate boundary beneath the Pacific Ocean. These shallow events are confined mainly to the so-called ‘granitic layer’ (Takagi *et al.* 1977). The accuracy of hypocentre locations of shallow events beneath the land area by the seismic network of Tohoku University has been much improved in the past three years. A detailed seismicity study made recently reveals that the cut-off depth for this shallow seismicity does not coincide with the Conrad depth (*ca.* 18 km beneath the northeastern Japan arc (Zhao *et al.* 1990)), but is slightly shallower than that. Figure 3 shows focal depth distribution of shallow micro-earthquakes accurately located in the land area of the northeastern Japan arc. Most of the shallow events (more than 98%) are found to be shallower than 15 km. The cut-off depth for this shallow seismicity, which is sharply delimited, can be interpreted as a brittle to ductile transition or a stick-slip to stable-sliding transition due to increasing temperature with depth (Brace & Byerlee 1970; Meissner & Strehlau 1982; Sibson 1982; Tse & Rice 1986). The upper 15 km of the crust forms a brittle seismogenic zone.

If examined in more detail, the cut-off depth for this shallow seismicity is found to vary with the location. Regional variations of the cut-off depth can be seen on figure 4. This figure shows a vertical cross section of shallow micro-earthquakes

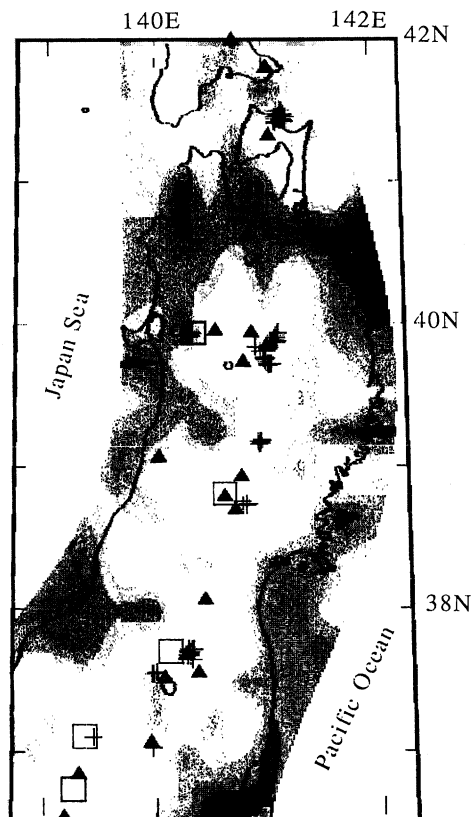


Figure 2. Fractional P -wave velocity perturbation (as %) at a depth of 40 km. Velocity perturbation is shown by the same light and shade scale as in figure 1. Solid triangles, crosses and open squares denote the locations of active volcanoes, low-frequency micro-earthquakes and S -wave reflectors, respectively.

within a 60 km width along the volcanic front accurately located in the central part of the northeastern Japan arc. Focal depths of all these events (except five anomalously deep events with low predominant frequencies) are shallower than about 15 km and their cut-off depth changes with location, becoming shallow beneath active volcanoes (solid triangles). The 3D P -wave velocity structure already described in §2 shows lower velocities in the crust beneath these active volcanoes than those beneath the other areas. The local elevation of the cut-off depth for the shallow seismicity near active volcanoes can be explained by the local elevation of the depth to the brittle to ductile (or stick-slip to stable-sliding) transition zone due to a higher temperature in the crust under those places.

4. Deep low-frequency micro-earthquakes beneath active volcanoes

Focal depth distributions of shallow events in the land area (figure 3) show that most events (more than 98%) occur in the upper 15 km of the crust, which forms a brittle seismogenic zone. However, exceptionally deep micro-earthquakes, well below the base of the brittle seismogenic zone, actually occur in the land area of the northeastern Japan arc, although the frequency of their occurrence is very low (0.97% of shallow events in the land area). These deep events can be seen in figure

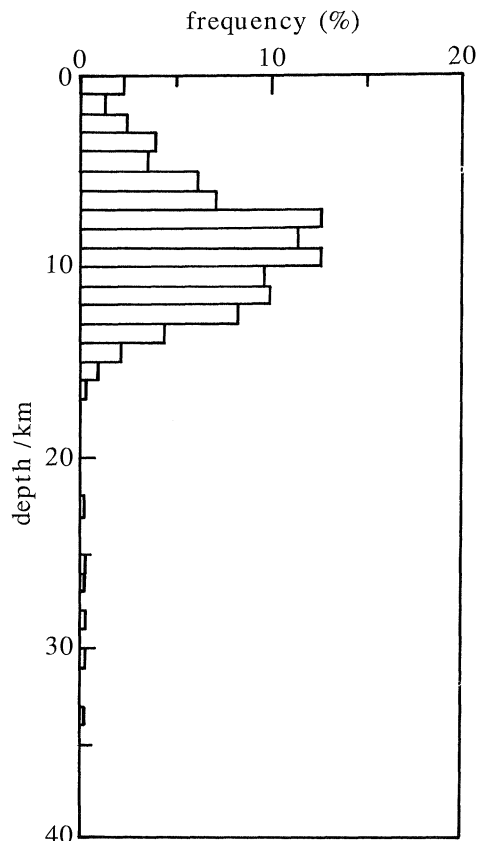


Figure 3. Depth-frequency distribution of shallow micro-earthquakes located in the land area of the northeastern Japan arc in November 1988 through April 1990.

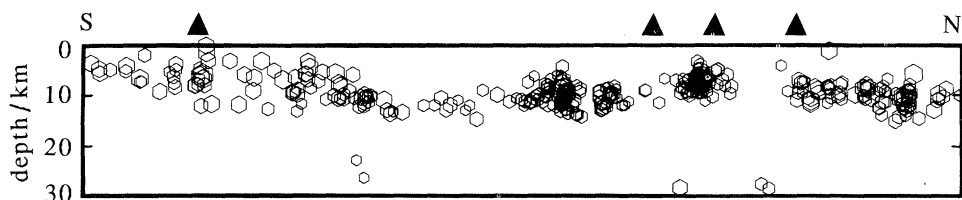


Figure 4. Vertical cross section of micro-earthquakes (open circles) within a 60 km width along the volcanic front located in the central part of the northeastern Japan arc in November 1989 through October 1991. Solid triangles on the top show the locations of active volcanoes.

3 as a distribution at depths greater than 22 km, which is distinctly isolated from the main activity shallower than 17 km. Five of the deep events are also seen on the vertical cross section in figure 4. We have so far found 151 deep events that occurred at 10 locations in the northeastern Japan arc. A detailed investigation of these deep events reveals that all of these events have the following anomalous features: (1) their focal depths are anomalously deep (22–40 km); (2) they have extremely low predominant frequencies (1.5–3.5 Hz) both for *P* and *S* waves; (3) their magnitudes are at most 2.5; (4) they have very long duration times of oscillations compared with events with normal focal depths; and (5) they occur around active volcanoes or around the *P*-wave low-velocity zones.

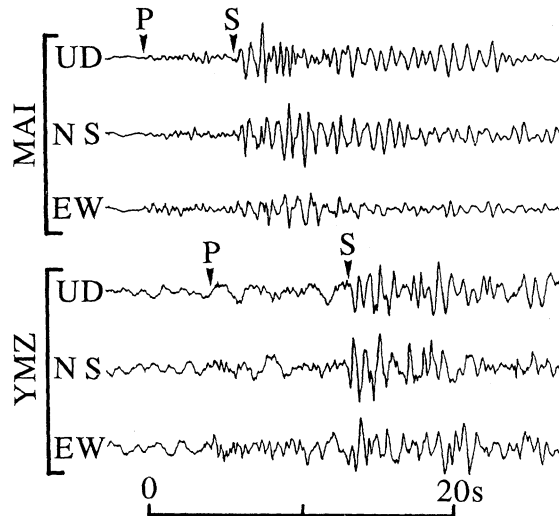


Figure 5. An example of three-component seismograms of a deep low-frequency micro-earthquake with magnitude of 1.8 that occurred beneath Hiuchidake volcano. Arrival times of direct P and S waves are denoted by P and S , respectively.

An example of three-component seismograms of a deep micro-earthquake recorded by short-period (1 s) seismometers is shown in figure 5. This shows seismograms of the deep event that occurred beneath Hiuchidake volcano in southwestern Fukushima Prefecture. The event has extremely low predominant frequencies both for P and S waves and very long duration times of oscillations.

All the 151 events detected at depths 22–40 km at 10 locations in the northeastern Japan arc are found to have extremely low predominant frequencies and long duration times. Earthquakes at depths 70–150 km, which occur in the deep seismic zone just under these low-frequency events, again have normal predominant frequencies both for P and S waves. Even if seismic waves from these earthquakes pass through the focal areas of the low-frequency events, their predominant frequencies are still normal. This means that the low predominant frequencies of these anomalously deep events are not caused by the path-effect.

Figure 6 shows the hypocentre distribution of the deep low-frequency events (open squares) that occurred at two locations near Kurikoma volcano (solid triangles) in southwestern Iwate Prefecture. Events with normal focal depths are also shown by open circles. All the events in this figure are those relocated by using the master-event method to improve the accuracy of hypocentre determinations. The low-frequency events shown by open squares are clearly isolated from the main activity of normal focal-depth events. This is common to all the low-frequency events that occurred at the other eight locations in the northeastern Japan arc, as can be estimated also from the focal depth distribution of shallow events in the land area (figure 3).

On the vertical cross sections in figure 1, the low-frequency events within a 60 km width along the lines AA', BB' and CC' in the inset map are plotted by solid circles. Epicentres of all the low-frequency events detected at 10 locations are plotted by crosses on the map of P -wave velocity distribution in figure 2. The low-frequency micro-earthquakes are located approximately beneath active volcanoes (solid triangles) or around the P -wave low-velocity zones (light areas).

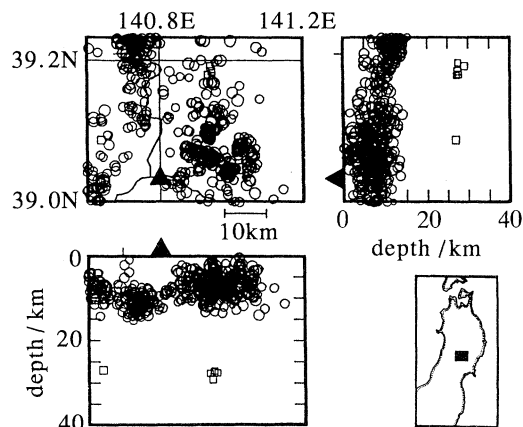


Figure 6. Hypocentre distribution of shallow micro-earthquakes (open circles) located near Kurikoma volcano in 1975–90. Low-frequency micro-earthquakes are shown by open squares. Solid triangles denote the location of Kurikoma volcano.

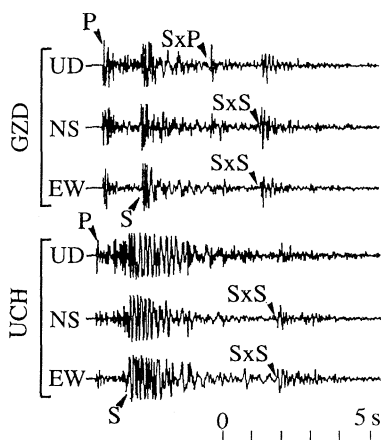


Figure 7. An example of three-component seismograms of a shallow event that occurred near Nikko-Shirane volcano. *P*- and *S*-wave first arrivals are denoted by *P* and *S*. Later arrivals are clearly seen and are indicated by *SxS* and *SxP*.

We have tried to estimate focal mechanisms of the low-frequency events by using initial motions of *P* waves, although the number of polarity data and their coverage on the focal sphere are not sufficient because of their small magnitudes. A relatively large event that occurred beneath Osoreyama volcano in northern Aomori Prefecture has a distribution of *P*-wave initial motions on the focal sphere inconsistent with a double-couple mechanism. A preliminary estimation by a moment-tensor inversion using first *P*- and *S*-wave amplitudes for this event also suggests a non-double-couple rather than a normal double-couple mechanism (Kosuga *et al.* 1991). The close locations of these anomalous events to active volcanoes and other features described above suggest that they are generated by magmatic activity, such as the rapid movement of magma, in the depth range from 22 to 40 km.

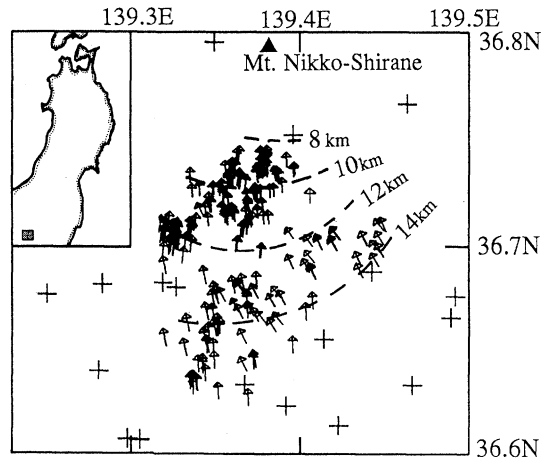


Figure 8. Geometry of the *S*-wave reflector beneath Nikko-Shirane volcano. The estimated depth to the reflector is shown by broken contours. Arrows denote the reflection points of observed reflected waves and the local upgrade directions of the reflector. Locations of observation stations temporarily deployed are shown by crosses.

5. Mid-crustal magma bodies estimated from *S*-wave reflections

Distinct *S*-wave reflections from shallow earthquakes have been found at five locations of the northeastern Japan arc. Figure 7 shows an example of three-component seismograms of a shallow micro-earthquake that occurred near Nikko-Shirane volcano in western Tochigi Prefecture. A sharp impulsive phase (denoted by '*SxS*' in the figure) following the direct *S* wave is recognized at two stations, which are located just above the hypocentre of this event. This unusual phase is most clearly defined on horizontal component seismograms and its amplitude is very large, in some cases being even larger than that of the direct *S* wave. Arrival time analysis indicates that this phase is an *S* wave reflected from a velocity discontinuity in the mid-crust (*SxS* phase). A reflected and *S* to *P* converted phase (*SxP* phase) at the same discontinuity is also detected as can be seen on the vertical component seismogram at one of the two stations shown in figure 7 (denoted by '*SxP*').

Figure 8 shows the estimated location of the *S*-wave reflector by analysing arrival times of the *SxS* phase observed by a dense seismic network temporarily deployed in this region (Matsumoto & Hasegawa 1991). The reflector has a shape similar to a section of a cone and is distributed over an area of $15 \times 10 \text{ km}^2$ at depths ranging from 8 to 15 km. It becomes shallow at an angle of about 30° toward the north, in which direction Nikko-Shirane volcano (solid triangle) is located.

Distinct *SxS* and *SxP* phases from a reflector in the mid-crust, similar to the present case, were first detected and identified beneath the Rio Grande Rift near Socorro, New Mexico (Sanford *et al.* 1973). The large amplitude of the *SxS* phase and *SxP* to *SxS* amplitude ratios are explained by a large velocity contrast across a discontinuity underlain by low-rigidity material, such as a magma body (Sanford *et al.* 1973). Observed spectral ratios of *SxS* to direct *S* phases have three peaks in the frequency range from 3 to 20 Hz, which can be explained by a very thin (thickness of *ca.* 100 m) magma body containing low-rigidity (*P*- and *S*-wave velocities of *ca.* 3 and 1 km s^{-1} , respectively) material (Matsumoto & Hasegawa 1991). A very thin magma body is partly supported by the following observation. Direct *S* waves

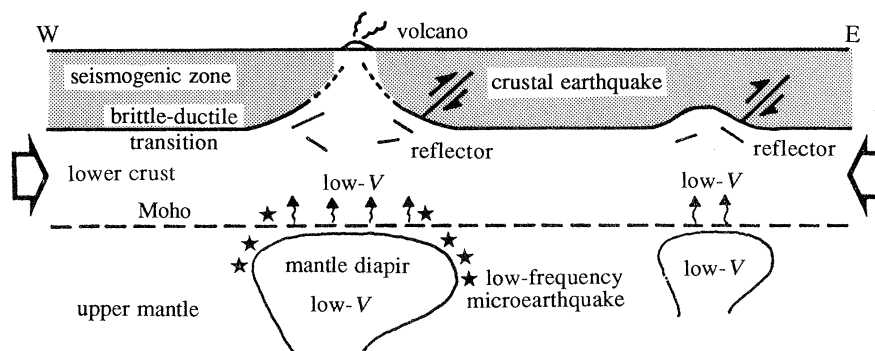


Figure 9. Schematic east-west cross section of the crust and upper mantle structure beneath the northeastern Japan arc.

observed at stations just above the magma body from earthquakes in the deep seismic zone right under it, which pass through the estimated magma body in the mid-crust, do not have spectra different from those at other stations. This indicates that S waves passing through the magma body are not attenuate significantly, suggesting that the thickness of the magma body is very thin, similar to that detected beneath the Rio Grande Rift, New Mexico (Ake & Sanford 1988).

Distinct S -wave reflectors in the mid-crust have been detected so far at five locations in the northeastern Japan arc (Mizoue *et al.* 1982; Horiuchi *et al.* 1988; Iwase *et al.* 1989; Hasegawa *et al.* 1991). Locations of the reflectors are plotted by large squares on the map of P -wave velocity distribution in figure 2. As is obvious from this figure, all the reflectors are located near active volcanoes (solid triangles) and/or in or around the low-velocity zones of P wave (light areas). Deep low-frequency micro-earthquakes (crosses) are distributed at greater depths (22–40 km) beneath the reflectors. These observations and the features of S_xS phase described above support the evidence that the S_xS and S_xP phases observed are reflected phases from thin magma bodies in the mid-crust.

6. Discussion and conclusions

We infer the structure of the crust and upper mantle beneath the northeastern Japan arc schematically as shown in figure 9, by combining the observations described in the previous sections (Hasegawa *et al.* 1991). The low-velocity zones inclined to the west in the upper mantle perhaps correspond to ascending flow of subduction-induced convection in the mantle wedge (Toksöz & Bird 1977). The migration of mass in the ascending flow causes upwelling of hot mantle material, and thus produces low-velocity zones which form roots of arc volcanoes at depth. Low-velocity zones just under the Moho discontinuity are the manifestation of mantle diapirs, and their magmatic activity (such as the rapid movement of magma) may generate low-frequency micro-earthquakes around them.

Molten material rising from the uppermost mantle makes its appearance in the mid-crust as distinct S -wave reflectors which are supposed to be very thin magma bodies. They also raise the temperature of crustal materials around them, causing the local elevation of the base of the brittle seismogenic zone. The lower portion of the crust and the mantle wedge, below the base of the seismogenic zone, are governed by creep and flow, because of a large geothermal gradient beneath this volcanic arc, and

they are incapable of supporting much stress (Shimamoto 1991). Most of the horizontal compressional stress as caused by subduction of the Pacific plate is supported by the upper 15 km of the crust which forms the brittle seismogenic zone. This situation causes stress concentration around places where the base of the seismogenic zone is locally elevated, and shallow crustal earthquakes occur in those places. Our interpretation seems to be supported in part by the fact that many large crustal earthquakes occur in or around the *P*-wave low-velocity zones (Hasegawa *et al.* 1991).

Spatial resolution of our *P*-wave tomographic inversion is 25–30 km (Zhao *et al.* 1992). The low-velocity zones in the uppermost mantle, which are supposed to be mantle diapirs, are just the images obtained with this resolution. Further investigation with much higher resolution would provide clearer images of them. Making use of reflected seismic waves is a powerful approach to the improvement of spatial resolution. Recently, in seismograms of shallow micro-earthquakes, we have detected a clear *S* wave reflected from a sharp velocity discontinuity in the uppermost mantle just beneath Osoreyama volcano in northern Aomori Prefecture (Hori & Hasegawa 1991). This distinct *S*-wave reflector is located over an area of $5 \times 5 \text{ km}^2$ at depths of 44–48 km within a *P*-wave low-velocity body of the uppermost mantle, and becomes shallow toward the north-northeast at an angle of about 40° . On the extension of it, low-frequency micro-earthquakes are distributed at depths of 25–35 km. Seismic observations for obtaining more detailed structure of mantle diapirs will make an important contribution to a better understanding of arc volcanism.

Finally, the deep structure of active volcanoes beneath the northeastern Japan arc obtained to date from seismic observations is summarized as follows. Clear *P*-wave low-velocity zones are found in the crust and in the mantle wedge. The low-velocity zones in the crust and the uppermost mantle just beneath active volcanoes are inclined to the west in the mantle wedge and attain a depth of about 150 km. Around the low-velocity zones there occur anomalously low-frequency micro-earthquakes at depths of 22–45 km, perhaps caused by magmatic activity in this depth range. Very thin magma bodies are found in or around the low-velocity zones at depths of 8–15 km in the mid-crust. A brittle seismogenic zone, corresponding to the upper 15 km of the crust, changes its thickness with the location, and its base is locally elevated just beneath active volcanoes.

References

- Ake, J. P. & Sanford, A. R. 1988 New evidence for the existence and internal structure of a thin layer of magma at mid-crustal depths near Socorro, New Mexico. *Bull. Seism. Soc. Am.* **78**, 1335–1359.
- Aki, K. & Lee, W. H. K. 1976 Determination of three-dimensional velocity anomalies under a seismic array using first *P* arrival times from local earthquakes. 1. A homogeneous initial model. *J. geophys. Res.* **81**, 4381–4399.
- Aki, K., Christofferson, A. & Husebye, E. S. 1977 Determination of the three-dimensional seismic structure of the lithosphere. *J. geophys. Res.* **82**, 277–296.
- Ando, M., Ishikawa, Y. & Yamazaki, F. 1983 Shear wave polarization anisotropy in the upper mantle beneath Honshu, Japan. *J. geophys. Res.* **88**, 5850–5864.
- Brace, W. F. & Byerlee, J. D. 1970 California earthquakes: why only shallow focus? *Science, Wash.* **168**, 1573–1575.
- Hasegawa, A., Umino, N. & Takagi, A. 1978 Double-planed deep seismic zone and upper mantle structure in the northeastern Japan arc. *Geophys. Jl R. astr. Soc.* **54**, 281–296.

- Hasegawa, A., Zhao, D., Hori, S., Yamamoto, A. & Horiuchi, S. 1991 Deep structure of the northeastern Japan arc and its relationship to seismic and volcanic activity. *Nature, Lond.* **352**, 683–689.
- Hasemi, A. H., Ishii, H. & Takagi, A. 1984 Fine structure beneath the Tohoku District, northeastern Japan arc, as derived by an inversion of *P*-wave arrival times from local earthquakes. *Tectonophys.* **101**, 245–265.
- Hori, S. & Hasegawa, A. 1991 Location of a mid-crustal magma body beneath Mt. Moriyoshi, northern Akita Prefecture, as estimated from reflected *SxS* phases. *J. Seism. Soc. Japan* **44**, 39–48.
- Hori, S. & Hasegawa, A. 1991 Anomalous *S*-wave reflector in the upper mantle beneath Osoreyama volcano. *Programme and Abstracts of Seism. Soc. Japan* no. 2, 208.
- Horiuchi, S., Hasegawa, A., Takagi, A., Ito, A., Suzuki, M. & Kameyama, H. 1988 Mapping of a melting zone near Mt. Nikko-Shirane in northern Kanto, Japan, as inferred from *SxP* and *SxS* reflections. *Tohoku Geophys. J.* **31**, 43–55.
- Hirahara, K., Ikami, A., Ishida, M. & Mikumo, T. 1989 Three-dimensional *P*-wave velocity structure beneath central Japan: low-velocity bodies in the wedge portion of the upper mantle above high-velocity subducting plates. *Tectonophys.* **163**, 63–73.
- Iwase, R., Urabe, S., Katsumata, K., Moriya, M., Nakamura, I. & Mizoue, M. 1989 Mid-crustal magma body in southwestern Fukushima Prefecture detected by reflected waves from microearthquakes. *Programme and Abstracts of Seism. Soc. Japan* no. 1, 185.
- Kosuga, M., Michinaka, M. & Hasegawa, A. 1991 Focal mechanism of low frequency earthquakes in the northeastern Japan arc. 1 Case study of the earthquakes in Shimokita region. *Abstracts for the 1991 Japan Earth and Planetary Science Joint Meeting*, 105.
- Matsumoto, S. & Hasegawa, A. 1991 Characteristics of mid-crustal *S*-wave reflector in Nikko-Ashio region. *Programme and Abstracts of Seism. Soc. Japan*, 204.
- Meissner, R. & Strehlau, J. 1982 Limits of stresses in continental crusts and their relation to the depth-frequency distribution of shallow earthquakes. *Tectonics* **1**, 73–89.
- Mizoue, M., Nakamura, I. & Yokota, T. 1982 Mapping of an unusual crustal discontinuity by microearthquake reflections in the earthquake swarm area near Ashio, northwestern part of Tochigi Prefecture, central Japan. *Bull. Earthquake Res. Inst.* **57**, 653–686.
- Obara, K., Hasegawa, A. & Takagi, A. 1986 Three-dimensional *P* and *S* wave velocity structure beneath the northeastern Japan arc. *J. Seism. Soc. Japan* **39**, 201–215.
- Sanford, A. R., Alptekin, O. & Topozada, T. R. 1973 Use of reflection phases on microearthquake seismograms to map an unusual discontinuity beneath the Rio Grande Rift. *Bull. Seism. Soc. Am.* **63**, 2021–2034.
- Sibson, R. H. 1982 Fault zone models, heat flow, and the depth distribution of earthquakes in the continental crust of the United States. *Bull. Seism. Soc. Am.* **72**, 151–163.
- Shimamoto, T. 1991 Rheology of rocks and plate tectonics – from rigid plates to deformable plates. *Comprehensive Rock Engng.* (Submitted.)
- Takagi, A., Hasegawa, A. & Umino, N. 1977 Seismic activity in the northeastern Japan arc. *J. Phys. Earth* **25**, 95–104.
- Toksöz, M. N. & Bird, P. 1977 Formation and evolution of marginal basins and continental plateaus. In *Island arcs, deep sea trenches and back-arc basins* (ed. M. Talwani & W. C. Pitman). AGU.
- Tse, S. T. & Rice, J. R. 1986 Crustal earthquake instability in relation to the depth variation of frictional slip properties. *J. geophys. Res.* **91**, 9452–9472.
- Zhao, D. & Hasegawa, A. 1992 *P*-wave tomographic imaging of the crust and upper mantle beneath the Japan Islands. *J. geophys. Res.* (In the press.)
- Zhao, D. & Hasegawa, A. & Horiuchi, S. 1992 Tomographic imaging of *P* and *S* wave velocity structure beneath northeastern Japan. *J. geophys. Res.* (In the press.)
- Zhao, D., Horiuchi, S. & Hasegawa, A. 1990 3-D seismic velocity structure of the crust and the uppermost mantle in the northeastern Japan arc. *Tectonophys.* **181**, 135–149.

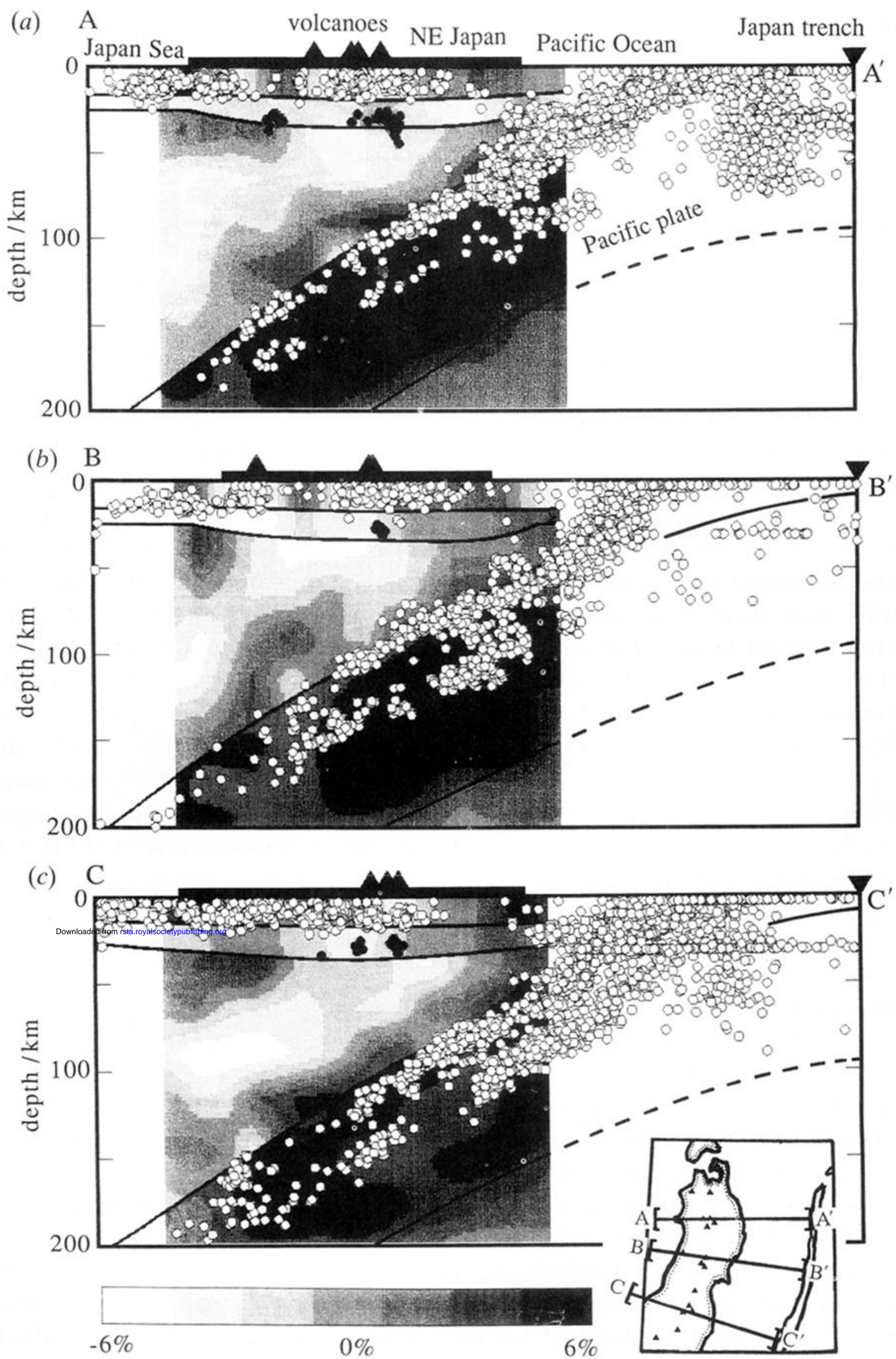


Figure 1. Vertical cross sections of fractional P -wave velocity perturbation (as %) along the lines (a) AA', (b) BB' and (c) CC' in the insert map. Velocity perturbation is shown by the light and shade scale at the bottom. Open circles are micro-earthquakes within a 60 km width along each line located in 1987–90, and solid circles denote low-frequency micro-earthquakes located in 1975–90. The locations of the land area, trench axis and active volcanoes are shown on the top by a thick horizontal line, inverted solid triangles and solid triangles, respectively. The Conrad and Moho discontinuities and the top of the subducted slab, which are fixed in the inversion, are shown by thick lines. The estimated location of the bottom of the slab is also shown by a thick line.

Downloaded from rsta.royalsocietypublishing.org

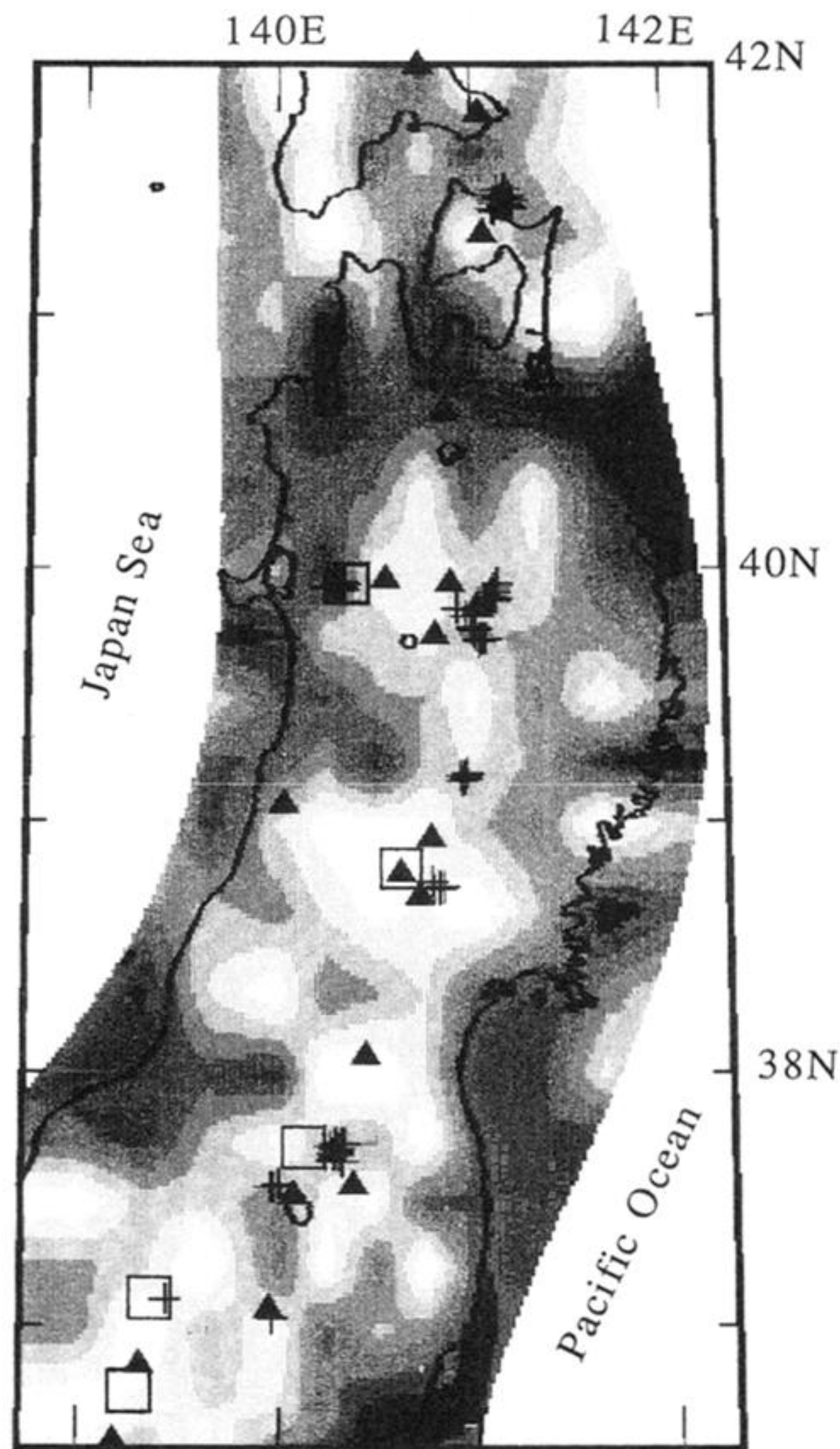


Figure 2. Fractional *P*-wave velocity perturbation (as %) at a depth of 40 km. Velocity perturbation is shown by the same light and shade scale as in figure 1. Solid triangles, crosses and open squares denote the locations of active volcanoes, low-frequency micro-earthquakes and *S*-wave reflectors, respectively.